Nonlinear Dyn (2018) 93:2169–2184
https://doi.org/10.1007/s11071-018-4317-8

ORIGINAL PAPER

General high-order rogue waves to nonlinear Schrödinger–Boussinesq equation with the dynamical analysis

Xiaoen Zhang · Yong Chen

Received: 19 March 2018 / Accepted: 4 May 2018 / Published online: 15 May 2018

Abstract General high-order rogue waves of the nonlinear Schrödinger–Boussinesq equation are obtained by the KP-hierarchy reduction theory, and the N-order rogue waves are expressed with the determinants, whose entries are all algebraic forms, which is shown in the theorem. It is found that the fundamental first-order rogue waves can be classified into three patterns: four-petal state, dark state, bright state by choosing different values of parameter α. An interesting phenomenon is discovered as the evolution of the parameter α: the rogue wave changes from four-petal state to dark state, whereafter bright state, which are consistent with the change in the corresponding critical points to the function of two variables. Furthermore, the dynamical property of second-order and third-order rogue waves is plotted, which can be regarded as the nonlinear superposition of the fundamental first-order rogue waves.

Keywords High-order rogue waves · Nonlinear Schrödinger–Boussinesq equation · KP-hierarchy reduction technique

The project is supported by the Global Change Research Program of China (No. 2015CB953904), National Natural Science Foundation of China (Nos. 11435005, 11675054), Shanghai Collaborative Innovation Center of Trustworthy Software for Internet of Things (No. ZF1213).

X. Zhang · Y. Chen (✉)
Shanghai Key Laboratory of Trustworthy Computing, East China Normal University, Shanghai 200062, China
e-mail: profchenyong@163.com

1 Introduction

Recently, there are many studies about the rogue waves on both experimental observation and theoretical analysis, which initially turn to describe the spontaneous ocean surface waves. The possible mechanisms of rogue waves generation consist of modulation instability [1,2], ripples interaction [3], the nonlinear focusing of the transient frequency modulation wave [4] and so on. The study of rogue waves is currently one of the hot topics encompassing many aspects, such as optics [5–7], Bose–Einstein condensates [8], plasma [9] and even finance [10]. Fundamentally, rogue wave is modeled as a transient wavepacket localized in both space and time. Aside from having a peak amplitude more than twice the background wave, it has a special feature with the instability and unpredictability. As a one-dimensional integrable scalar equation to display the nonlinear wave propagation, the nonlinear Schrödinger equation (NLS) [11–18] plays a key role in the description of rogue waves, which has various applications related from the deep water hydrodynamics to nonlinear optics. In 1983, Peregrine [19] first gave a rational rogue waves to the NLS equation, whose generation principle is identified as the evolution of the breather when the period tends to infinity. The rogue wave-peregrine soliton was observed through the experiment in the optics [5] and in the tank [20]. It is well known that rogue waves have different spatial–temporal structures, for example, the eye-shaped pattern can be found in the scalar equation while the anti-eye-shaped and four-petals [21] in the vector ones. The understanding of the fundamental first-order rogue waves is crucial to the dynamics property because the corresponding high-order rogue waves can be regarded as the nonlinear superposition of the fundamental rogue waves and exhibit higher peak amplitude. It is meaningful to study the high-order rogue wave because the high-order rogue wave can be regarded as a kind of rogue waves with higher ratio of peak to the background amplitude. By using the Darboux transformation, the significant fourth-order rogue wave was provided on the theoretically by Akhmediev [12]. Chabchoub et al. observed the fifth-order rogue wave in the water tank [22].

Another significant research on the rogue waves is the multicomponent coupled system, which can appear some more exciting dynamical characters consisted of three kinds of interactions among rogue waves, breather and soliton: the interaction between the same, two different or even three different states, due to the increase in the degrees of freedom. For instance, for the coupled NLS equation [23,24], it appears the dark rogue waves, the interactions between the rogue waves and other localized waves because the relative velocity cannot be affected by any trivial changes. The interactions between high-order rogue waves and other localized waves are presented by using the Darboux transformation [25,26] or Hirota bilinear method [27]. Apart from the multicomponent coupled system, the high-dimensional system can describe the rogue waves more verisimilitude. We found the rogue wave aroused by the lump soliton and a pair of resonance stripe solitons, which is different from the traditional high-dimensional line rogue wave and refers to the KP equation [28], the Jimbo–Miwa equation [29] and $(2+1)$-dimensional KdV equation [30].

The KP-hierarchy reduction technique is very powerful to investigate the integrable system and derive the localized waves. It was established by the Kyoto School [31,32] in 1980s to get the soliton solution of integrable system. Based on this technique, Ohta et al. obtained the N-dark–dark soliton solution of a two-coupled NLS equation [33] in 2012. In 2014, Feng constructed the general bright–dark soliton solutions coupled with all combinations to the NLS equation [34]. Meanwhile, Ling et al. obtained the multi-dark soliton for N-component nonlinear Schrödinger equations by using Darboux transformation [35]. Recently, the Yajima–Oikawa system (also can be called the long wave–short wave interaction equation) [36–39] and Mel'nikov system (also can be called NLS-KP equation) [40–42] were studied through the KP-hierarchy reduction technique. In terms of the Yajima–Oikawa equation, its high-order rogue waves and rational solutions were obtained. Similarly, the N-dark soliton solution, bright–dark mixed N-soliton solutions to the Mel'nikov systems were given.

Based on the KP-hierarchy reduction technique, we construct the general high-order rogue waves to the NLS-Boussinesq equation,

$$\begin{aligned} & i\Phi_t - \Phi_{xx} - u\Phi = 0, \\ & u_{xx} + u_{xxxx} + 3(u^2)_{xx} - 3u_{tt} + (\Phi\Phi^*)_{xx} = 0, \end{aligned} \tag{1}$$

where Φ is a complex function, Φ^* is the complex conjugate function of Φ, and u is a real function. This system is used to describe the nonlinear propagation of the coupled Langmuir and dust-acoustic waves, including some ions, electrons and massive charged dust particles. For slow modulations, the amplitude of Langmuir wave can be dominated by the NLS equation, while for the small but finite amplitude ion-acoustic wave, it must be governed by a driven Boussinesq equation to display a bidirectional propagation. There are many studies to Boussinesq equation [43] or its recombined equations [44]. Generally speaking, NLS equation can be used to describe the Langmuir wave and the linear equation can be used to depict the dust-acoustic waves accompanying with small-amplitude. However, when the propagation wave is located in the near of the dust-acoustic with a finite amplitude, the linear equation will not describe this phenomenon precisely, instead, this phenomenon can be governed by the nonlinear Boussinesq equation. This equation was first be given in [45], then its analytical solution, N-soliton solutions and other patterns were reported in [46–48]. Recently, time-fractional Boussinesq equation [49] becomes a hot point for Rossby solitary waves in fluid, maybe the time-fractional NLS-Boussinesq equation will have more research value.

In this paper, we mainly discuss the general high-order rogue waves to the NLS-Boussinesq equation by using the KP-hierarchy reduction technique. To our knowledge, the high-order rogue waves of the NLS-Boussinesq equation are never obtained. We give the general formula of the N-order rogue waves in the theorem and prove it by the lemma. The obtained rogue waves can be classified as three patterns, four-petal state, dark state and bright state. As the evolution of the parameter α, the rogue wave turns from the four-petal state to the dark state until to the bright state, the progress can be explained through the critical points property to the function with two variables, that is, if there are four critical points, two are maximums and two the minimums, it is the four-petal state; if there are three critical points, one is minimum and two the maximums, it is the dark state; otherwise, one is maximum and two minimums, it is the bright state. Since the conversion between different states can be governed by a free parameter α, which is meaningful to the transformation between different states in the experiment. The rich dynamical behaviors are shown through some figures. In Ref. [21], the authors demonstrated that these rogue waves in the two-coupled NLS equation can be transited to each other; in other words, the four-petal rogue wave can be changed into the bright state or the dark state with the varying of the relative frequency. However, in our paper, the four-petal state cannot be changed into the bright; perhaps, the reason is that the relative amplitude of these two minimums is bigger than that of these two maximums no matter how the parameter α transform. Then, the dynamical behavior of second-order and third-order rogue waves is shown in the figures.

The structure of this paper is organized as follows: Sect. 2 lists some KP-hierarchy with Gram determinant and reduce the bilinear KP-hierarchy into the bilinear equation of the NLS-Boussinesq by some parameter constraints, in which the elements of this equation are algebraic expression. The dynamical first-order fundamental rogue waves, high-order rogue waves and the corresponding analysis are presented in Sect. 3. The last section is the conclusion and some summary.

2 The bilinear form of NLS-Boussinesq equation derived from the KP-hierarchy

We obtain the bilinear form of Eq. (1) connected with the famous KP-hierarchy in this section, which is crucial to derive the fundamental rogue waves and high-order rogue waves. Let us introduce the following variable transformation

$$\Phi = e^{\mathrm{i}(\alpha x+\alpha^2 t)}\frac{g}{f}, \qquad u = 2\frac{\partial^2}{\partial x^2}\log f$$

where α is an arbitrary real constant, f is a real-value function, and g is a complex-valued function. Under this transformation, the NLS-Boussinesq equation can be transferred to its bilinear form

$$\begin{aligned}&\left(\mathrm{i}D_t - 2\mathrm{i}\alpha D_x - D_x^2\right) g\cdot f = 0,\\ &\left(D_x^2 + D_x^4 - 3D_t^2 - 1\right) f\cdot f + gg^* = 0,\end{aligned} \tag{2}$$

where g^* is the complex conjugate of g and D is the bilinear operator defined as

$$\begin{aligned}&D_t^m D_x^n(a,b)\\ &\quad\equiv \frac{\partial^m}{\partial s^m}\frac{\partial^m}{\partial y^m}a(t+s,x+y)b(t-s,x-y)\Big|_{s=0,y=0}.\end{aligned}$$

It needs to some skills to obtain the polynomial solutions of f and g by using the τ function of KP-hierarchy under the reduction. We will give prominence to the steps of the derivation in detail, which is shown in the next.

Firstly, we list three bilinear equations from the KP-hierarchy

$$\begin{aligned}&\left(D_{x_1}^2 + 2aD_{x_1} - D_{x_2}\right)\tau(k+1,l)\cdot\tau(k,l) = 0,\\ &\left(\frac{1}{2}D_{x_1}D_{x_{-1}} - 1\right)\tau(k,l)\\ &\quad\cdot\tau(k,l) + \tau(k+1,l)\cdot\tau(k-1,l) = 0,\\ &\left(D_{x_1}^4 - 4D_{x_1}D_{x_3} + 3D_{x_2}^2\right)\tau(k,l)\cdot\tau(k,l) = 0,\end{aligned} \tag{3}$$

they have been proved to have the following Gram determinant solutions in Ref. [40],

$$\tau(k,l) = |m_{ij}(k,l)|_{1\le i,j\le N}, \tag{4}$$

and the elements are given

$$\begin{aligned}&m_{ij}(k,l) = c_{ij} + \int \phi_i(k,l)\psi_j(k,l)\mathrm{d}x_1,\\ &\phi_i(k,l) = (p_i - a)^k \exp(\xi_i),\\ &\psi_j(k,l) = \left(\frac{-1}{q_j + a}\right)^k \exp(\tilde{\xi}_j),\end{aligned}$$

where ξ_i and $\tilde{\xi}_j$ are functions of the variables x_{-1}, x_1, x_2, x_3, which can be written as

$$\xi_i = \frac{1}{p_i - a}x_{-1} + p_i x_1 + p_i^2 x_2 + p_i^3 x_3 + \xi_{i0},$$
$$\tilde{\xi}_j = \frac{1}{q_j + a}x_{-1} + q_j x_1 - q_j^2 x_2 + q_j^3 x_3 + \tilde{\xi}_{i0}.$$

Since these bilinear equations contain more than two variables, we hope to look for an algebraic solutions satisfying the reduction

$$\left(\partial_{x_3} - \frac{1}{8}\partial_{x_{-1}} + \frac{1}{4}\partial_{x_1}\right)\tau(k,l) = c\tau(k,l), \tag{5}$$

so as to convert the bilinear KP-hierarchy into the $(1+1)$-dimensional bilinear equations

$$\begin{aligned} &\left(D_{x_1}^2 + 2aD_{x_1} - D_{x_2}\right)\tau(k+1,l)\cdot\tau(k,l) = 0, \\ &\left(D_{x_1}^2 + D_{x_1}^4 + 3D_{x_2}^2 - 1\right)\tau(k,l) \\ &\quad\cdot\tau(k,l) + \tau(k+1,l)\cdot\tau(k-1,l) = 0. \end{aligned} \tag{6}$$

Secondly, by defining $f = \tau(0,0)$, $g = \tau(1,0)$, $h = \tau(-1,0)$, $a = \mathrm{i}\alpha$ and with the variables transformation:

$$x_1 = x, x_2 = \mathrm{i}t$$

Equation (6) will be transferred into

$$\begin{aligned} &\left(D_x^2 + 2\mathrm{i}\alpha D_x - \mathrm{i}D_t\right)g\cdot f = 0, \\ &\left(D_x^2 + D_x^4 - 3D_t^2 - 1\right)f\cdot f + g\cdot h = 0. \end{aligned} \tag{7}$$

Then, we can obtain the bilinear form of $(1+1)$-dimensional NLS-Boussinesq equation under the real and complex conjugate condition:

$$f = \tau(0,0), \quad g = \tau(1,0), \quad g^* = h = \tau(-1,0)$$

Finally, the algebraic solution of $(1+1)$-dimensional NLS-Boussinesq equation can be presented according to its bilinear form.

3 The algebraic solution to the $(1+1)$-dimensional NLS-Boussinesq equation

In this section, we construct the algebraic solution from the classical KP-hierarchy, that is, reduction condition Eq. (5) must be satisfied. The detailed steps will be given in the lemma.

Lemma *Assume the element of the matrix m is the following form*

$$m_{kl}^{(\mu\nu n)} = \left(A_k^{(\mu)}B_l^{(\nu)}m^{(n)}\right)\Big|_{p=\theta,q=\theta^*}$$

where

$$\begin{aligned} m^{(n)} &= \frac{1}{p+q}\left(-\frac{p-a}{q+a}\right)^n e^{\eta+\tilde{\eta}}, \eta \\ &= px_1 + p^2x_2, \tilde{\eta} = qx_1 - q^2x_2, \end{aligned}$$

θ is a solution of the quadratic dispersion equation

$$\begin{aligned} &3(\theta-a)^3 + 6a(\theta-a)^2 + \left(3a^2 + \frac{1}{4}\right)(\theta - a) \\ &\quad + \frac{1}{8(\theta-a)} = 0, \end{aligned} \tag{8}$$

and $A_k^{(\mu)}, B_l^{(\nu)}$ are two differential operator with respect to p and q, defined by

$$\begin{aligned} A_k^{(\mu)} &= \sum_{j=0}^{k} a_j^{(\mu)}\frac{\left[(p-a)\partial_p\right]^{k-j}}{(k-j)!}, \quad k \geq 0, \\ B_l^{(\nu)} &= \sum_{j=0}^{l} b_j^{(\nu)}\frac{\left[(q+a)\partial_q\right]^{l-j}}{(l-j)!}, \quad l \geq 0, \end{aligned} \tag{9}$$

where the coefficients a_j^{μ}, b_j^{ν} satisfy

$$
\begin{aligned}
a_j^{(\mu+1)} &= \sum_{r=0}^{j} \frac{3^{r+2}(p-a)^3+3a2^{r+2}(p-a)^2+\left(\frac{12a^2+1}{4}\right)(p-a)+(-1)^{r+1}\frac{1}{8(p-a)}}{(r+2)!} \\
&\quad a_{j-r}^{(\mu)}, \mu=0,1,2\ldots \\
b_j^{(\nu+1)} &= \sum_{r=0}^{j} \frac{3^{r+2}(q+a)^3-3a2^{r+2}(q+a)^2+\left(\frac{12a^2+1}{4}\right)(q+a)+(-1)^{r+1}\frac{1}{8(p-a)}}{(r+2)!} \\
&\quad b_{j-r}^{(\mu)}, \nu=0,1,2\ldots
\end{aligned} \tag{10}
$$

then the solution of bilinear equation (7) can be written as

$$
\tau_n = \det_{1\le i,j\le N} = \begin{vmatrix} m_{11}^{(N-1,N-1,n)} & m_{13}^{(N-1,N-2,n)} & \cdots & m_{1,2N-1}^{(N-1,0,n)} \\ m_{31}^{(N-2,N-1,n)} & m_{33}^{(N-2,N-2,n)} & \cdots & m_{3,2N-1}^{(N-2,0,n)} \\ \vdots & \vdots & \vdots & \\ m_{2N-1,1}^{(0,N-1,n)} & m_{2N-1,3}^{(0,N-2,n)} & \cdots & m_{2N-1,2N-1}^{(0,0,n)} \end{vmatrix} \tag{11}
$$

The proof of this lemma is given in "Appendix A".

4 Complex conjugate condition and regularity

It has been proved that τ_n is the solution to the bilinear equation in the lemma, if the variables x_1, x_2 satisfy the following reduction

$$
x_1 = x, x_2 = -it, \tag{12}
$$

and the variable values of $a_k^{(0)}$ and $b_k^{(0)}$ are complex conjugate each other, then the recurrence values $a_k^{(\mu)}$ and $b_k^{(\mu)}$ will also be complex conjugate each other under the condition $p=\theta, q=\theta^*$, that is

$$
b_k^{\mu}|_{q=\theta^*} = \left(a_k^{(\mu)}|_{p=\theta}\right)^* \tag{13}
$$

for $\mu = 1, 2, \ldots, n$, then the matrix term

$$
\begin{aligned}
m_{kj}^{(\mu,\nu,n)*} &= m_{kj}^{(\mu,\nu,n)}\big|_{a_k^{(\mu)}\leftrightarrow b_k^{(\mu)}, x_2\leftrightarrow -x_2, a\leftrightarrow -a, \theta\leftrightarrow\theta^*} \\
&= m_{jk}^{(\mu,\nu,-n)},
\end{aligned} \tag{14}
$$

which indicates

$$
\tau_n^* = \tau_{-n}. \tag{15}
$$

It is well known that $f=\tau_0$, $g=\tau_1$, $g^*=\tau_{-1}$ are the solution of (1 + 1)-dimensional NLS-Boussinesq equation

$$
\begin{aligned}
&\left(\mathrm{i}D_t - 2\mathrm{i}\alpha D_x - D_x^2\right) g\cdot f = 0, \\
&\left(D_x^2 + D_x^4 - 3D_t^2 - 1\right) f\cdot f + gg^* = 0.
\end{aligned} \tag{16}
$$

Next, we show the rational function $\frac{g}{f}$ is nonsingular. According to the definition of $f=\tau_0$, it is found that f is a determinant of a Hermitian matrix $\tau_0 = \det(m_{2i-1,2j-1}^{(N-i,N-j,0)})$. In Ref. [11], it has been proved that when the real part of p is positive, $\tau_0 > 0$, conversely, when the real part is negative, $\tau_0 < 0$. Hence, whether the real part of p is positive or negative, the corresponding function τ_0 is always nonsingular.

Based on the proof in "Appendix A", we can obtain the general high-order rogue waves to the (1 + 1)-dimensional NLS-Boussinesq equation, which is shown in the theorem.

Theorem *The solution of the (1+1)-dimensional NLS-Boussinesq equation is*

$$
\begin{aligned}
\Phi &= e^{i(\alpha x+\alpha^2 t)}\frac{\tau_1}{\tau_0}, \\
u &= 2\frac{\partial^2}{\partial x^2} log\tau_0,
\end{aligned} \tag{17}
$$

where

$$\tau_n = \det_{1\le i,j\le N}\left(m_{2i-1,2j-1}^{(N-i,N-j,n)}\right) = \begin{vmatrix} m_{11}^{(N-1,N-1,n)} & m_{13}^{(N-1,N-2,n)} & \cdots & m_{1,2N-1}^{(N-1,0,n)} \\ m_{31}^{(N-2,N-1,n)} & m_{33}^{(N-2,N-2,n)} & \cdots & m_{3,2N-1}^{(N-2,0,n)} \\ \vdots & \vdots & \vdots & \\ m_{2N-1,1}^{(0,N-1,n)} & m_{2N-1,3}^{(0,N-2,n)} & \cdots & m_{2N-1,2N-1}^{(0,0,n)} \end{vmatrix}, \tag{18}$$

with $f = \tau_0$, $g = \tau_1$, $g^* = \tau_{-1}$, *and the entries of matrix* $m_{ij}^{(\mu,\nu,n)}$ *are defined by*

$$m_{ij}^{(\mu,\nu,n)} = \sum_{k=0}^{i}\sum_{l=0}^{j} \frac{a_k^{\mu}}{(i-k)!}\frac{a_l^{\nu *}}{(j-l)!} \left[(p-a)\partial_p\right]^{i-k}\left[(q+a)\partial_q\right]^{j-l} \frac{1}{p+q}\left(-\frac{p-a}{q+a}\right)e^{(p+q)x-(p^2-q^2)it}\Big|_{p=\theta,q=\theta^*} \tag{19}$$

where θ *is the solution of the quadratic dispersion equation*

$$3(\theta-a)^3 + 6a(\theta-a)^2 + \left(3a^2+\frac{1}{4}\right)(\theta-a) + \frac{1}{8(\theta-a)} = 0, \tag{20}$$

and a_k^{μ} *satisfies the recurrence relation*

$$a_j^{(\mu+1)} = \sum_{r=0}^{j} \frac{3^{r+2}(p-a)^3+3a2^{r+2}(p-a)^2+\left(\frac{12a^2+1}{4}\right)(p-a)+(-1)^{r+1}\frac{1}{8(p-a)}}{(r+2)!} a_{j-r}^{(\mu)},\ \mu = 0,1,2,\ldots \tag{21}$$

$$3(p-a)^3 + 6a(p-a)^2 + \left(3a^2+\frac{1}{4}\right)(p-a) + \frac{1}{8(p-a)} = 0, \tag{22}$$

this equation includes four roots as follows when $a = i\alpha$:

$$p_1 = \frac{\mathrm{i}\alpha}{2} + \frac{k_5^{\frac{1}{2}}}{12} + \frac{1}{12}\left(\frac{36\mathrm{i}\alpha}{k_5^{\frac{1}{2}}} - \frac{144\alpha^4-24\alpha^2+73}{k_3^{\frac{1}{3}}} - 24\alpha^2 - k_3^{\frac{1}{3}} - 4\right)^{\frac{1}{2}},$$

$$p_2 = \frac{\mathrm{i}\alpha}{2} + \frac{k_5^{\frac{1}{2}}}{12} - \frac{1}{12}\left(\frac{36\mathrm{i}\alpha}{k_5^{\frac{1}{2}}} - \frac{144\alpha^4-24\alpha^2+73}{k_3^{\frac{1}{3}}} - 24\alpha^2 - k_3^{\frac{1}{3}} - 4\right)^{\frac{1}{2}},$$

$$p_3 = \frac{\mathrm{i}\alpha}{2} - \frac{k_5^{\frac{1}{2}}}{12} + \frac{1}{12}\left(\frac{36\mathrm{i}\alpha}{-k_5^{\frac{1}{2}}} - \frac{144\alpha^4-24\alpha^2+73}{k_3^{\frac{1}{3}}} - 24\alpha^2 - k_3^{\frac{1}{3}} - 4\right)^{\frac{1}{2}},$$

$$p_4 = \frac{\mathrm{i}\alpha}{2} - \frac{k_5^{\frac{1}{2}}}{12} - \frac{1}{12}\left(\frac{36\mathrm{i}\alpha}{-k_5^{\frac{1}{2}}} - \frac{144\alpha^4-24\alpha^2+73}{k_3^{\frac{1}{3}}} - 24\alpha^2 - k_3^{\frac{1}{3}} - 4\right)^{\frac{1}{2}}, \tag{23}$$

where

$$k_1 = 3456\alpha^6 - 2592\alpha^4 + 2952\alpha^2 - 1058,$$
$$k_2 = -1728\alpha^6 + 432\alpha^4 - 1332\alpha^2 - 215,$$
$$k_3 = k_2 + 18k_1^{\frac{1}{2}},$$
$$k_4 = 144\alpha^4 - 12\alpha^2 k_3^{\frac{1}{3}} + k_3^{\frac{2}{3}} - 24\alpha^2 - 2k_3^{\frac{1}{3}} + 73,$$

5 General high-order rogue waves to NLS-Boussinesq equation

During the generation of rogue waves, a critical parameter a plays an important role to the pattern of rogue waves. Under the reduction, this parameter is a pure imaginary $\mathrm{i}\alpha$. In this section, we will discuss the dynamics properties detailedly. We first study the solution of the quadratic dispersion equation

$$k_5 = \frac{k_4}{k_3^{\frac{1}{3}}}. \tag{24}$$

Due to the complexity of the solutions, we cannot divide the real part from the corresponding solutions. So we give the first-order rogue waves based on Eq. (18) and discuss the effect of the parameter α on the pattern of the rogue waves. For simplicity, let $a_0^{(0)} = 1, a_1^{(0)} = 0, N = 1$, then the functions f and g can be written as

$$\begin{aligned} f &= \frac{e^{2\kappa(2\gamma t+x)}\left[\left(\kappa x + 2\gamma\kappa t - \frac{1}{2}\right)^2 + (2\kappa^2 t)^2 + \frac{1}{4}\right]\left[(\alpha-\gamma)^2+\kappa^2\right]}{2\kappa^3}, \\ g &= \frac{e^{2\kappa(2\gamma t+x)}\left[\left(m_1\kappa x+2\kappa m_3 t+\frac{\gamma-\alpha-\kappa+2i\kappa}{2}\right)^2 + \left(m_2\kappa x+2\kappa m_4 t+\frac{\gamma-\alpha+\kappa+2i\kappa}{2}\right)^2 + \frac{\kappa^2+(\alpha+\gamma)^2}{2}\right](i\kappa-\gamma+\alpha)}{4\kappa^3\,(i\kappa+\gamma-\alpha)} \end{aligned} \tag{25}$$

$$\begin{aligned} m_1 &= \alpha+\kappa-\gamma, \\ m_2 &= \alpha-\kappa-\gamma, \\ m_3 &= \kappa^2+2\kappa\gamma-\gamma^2+\alpha\gamma-\alpha\kappa, \\ m_4 &= \kappa^2-2\kappa\gamma-\gamma^2+\alpha\gamma+\alpha\kappa, \end{aligned}$$

where κ is the real part of p and γ is the imaginary part.

Then the first-order rogue wave to NLS-Boussinesq equation is

$$\begin{aligned} \Phi &= e^{\mathrm{i}(\alpha x+\alpha^2 t)}\frac{g}{f}, \\ u &= 2\frac{\partial^2}{\partial x^2}\log f \end{aligned} \tag{26}$$

where f, g is in Eq. (25).

With the simplify calculation, the modular square of the short-wave component $|\Phi|^2$ has five critical points:

$$\begin{aligned} (x_1,t_1) &= \left(\frac{1}{2\kappa}, 0\right), \\ (x_2,t_2) &= \left(\frac{(\alpha-2\gamma)\left(3\varpi^2-\kappa^2\right)^{\frac{1}{2}}+\varpi^2+\kappa^2}{2\kappa\left(\varpi^2+\kappa^2\right)}, \frac{\left(3\varpi^2-\kappa^2\right)^{\frac{1}{2}}}{4\kappa\left(\varpi^2+\kappa^2\right)}\right), \\ (x_3,t_3) &= \left(\frac{(2\gamma-\alpha)\left(3\varpi^2-\kappa^2\right)^{\frac{1}{2}}+\varpi^2+\kappa^2}{2\theta\left(\varpi^2+\kappa^2\right)}, \frac{\left(3\varpi^2-\kappa^2\right)^{\frac{1}{2}}}{-4\kappa\left(\varpi^2+\kappa^2\right)}\right), \\ (x_4,t_4) &= \left(\frac{\left(\alpha\gamma-\gamma^2+\kappa^2\right)\left(3\kappa^2-\varpi^2\right)^{\frac{1}{2}}+\kappa\left(\varpi^2+\kappa^2\right)}{2\kappa^2\left(\varpi^2+\kappa^2\right)},\right. \\ &\qquad \left.\frac{(\gamma-\alpha)\left(3\kappa^2-\varpi^2\right)^{\frac{1}{2}}}{4\kappa^2\left(\varpi^2+\kappa^2\right)}\right), \\ (x_5,t_5) &= \left(\frac{\left(\gamma^2-\alpha\gamma-\kappa^2\right)\left(3\kappa^2-\varpi^2\right)^{\frac{1}{2}}+\kappa\left(\varpi^2+\kappa^2\right)}{2\kappa^2\left(\varpi^2+\kappa^2\right)},\right. \\ &\qquad \left.-\frac{(\gamma-\alpha)\left(3\kappa^2-\varpi^2\right)^{\frac{1}{2}}}{4\kappa^2\left(\varpi^2+\kappa^2\right)}\right). \end{aligned} \tag{27}$$

where $\varpi = \alpha - \gamma$. According to the Hessian matrix with two variables at these critical points, the first-order cofactor is

$$\begin{aligned} H_1(x,t) &= \left[\frac{\partial^2|\Phi|^2}{\partial x^2}\right], \\ H_1(x_1,t_1) &= \frac{192\kappa^4\left[(\alpha-\gamma)^2-\kappa^2\right]}{\left[(\alpha-\gamma)^2+\kappa^2\right]} \\ H(x_2,t_2) &= H(x_3,t_3) = -\frac{6\kappa^4\left[(\alpha-\gamma)^2+\kappa^2\right]}{(\alpha-\gamma)^4} \\ H(x_4,t_4) &= H(x_5,t_5) = 6\left[(\alpha-\gamma)^2+\kappa^2\right] \end{aligned} \tag{28}$$

and the second-order cofactor is

$$\begin{aligned} H(x,t) &= \left[\frac{\partial^2|\Phi|^2}{\partial x^2}\frac{\partial^2|\Phi|^2}{\partial t^2} - \left(\frac{\partial^2|\Phi|^2}{\partial x\partial t}\right)^2\right] \\ H(x_1,t_1) &= \frac{16384\kappa^{10}\left[(\alpha-\gamma)^2-3\kappa^2\right]\left[3(\alpha-\gamma)^2-\kappa^2\right]}{\left[(\alpha-\gamma)^2+\kappa^2\right]^4}, \\ H(x_2,t_2) &= H(x_3,t_3) \\ &= \frac{64\kappa^{10}\left[3(\alpha-\gamma)^2-\kappa^2\right]\left[(\alpha-\gamma)^2+\kappa^2\right]^2}{(\gamma-\alpha)^{10}}, \\ H(x_4,t_4) &= H(x_5,t_5) \\ &= -64\left[(\alpha-\gamma)^2+\kappa^2\right]^2\left[(\alpha-\gamma)^2-3\kappa^2\right]. \end{aligned} \tag{29}$$

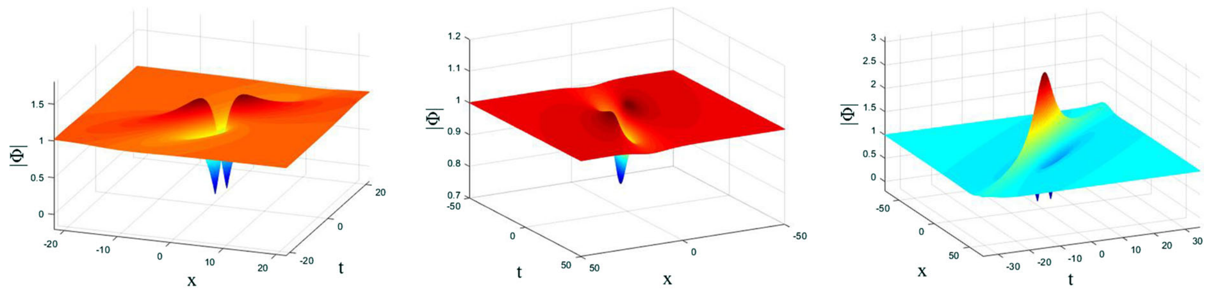

Fig. 1 (Color online) First-order rogue waves of NLS-Boussinesq equation: **a** four-petal state $\alpha = 0$, **b** dark state $\alpha = \frac{1}{2}$, **c** bright state $\alpha = \frac{\sqrt{3}}{2}$

Again, we begin to discuss the solution of Eq. (22). We only consider the positive value of parameter α because the negative value has the similar property.

When $k_1 > 0$, that is $\alpha > \left(\frac{\left(107+51\sqrt{17}\right)^{\frac{1}{3}}}{12} - \frac{8}{3\left(107+51\sqrt{17}\right)^{\frac{1}{3}}} + \frac{1}{4}\right)^{\frac{1}{2}}$, the imaginary part of p_1 is $\frac{\alpha}{2} + \frac{(-k_5)^{\frac{1}{2}}}{12}$, the real part is $\frac{1}{12}\left(\frac{36\mathrm{i}\alpha}{\sqrt{k_5}} - \frac{144\alpha^4 - 24\alpha^2 + 73}{k_3^{\frac{1}{3}}} - 24\alpha^2 - k_3^{\frac{1}{3}} - 4\right)^{\frac{1}{2}}$, and p_2 is the conjugate of p_1, but we cannot give the exact real part and imaginary part for both p_3 and p_4.

When $k_1 < 0$, that is $0 \le \alpha < \left(\frac{\left(107+51\sqrt{17}\right)^{\frac{1}{3}}}{12} - \frac{8}{3\left(107+51\sqrt{17}\right)^{\frac{1}{3}}} + \frac{1}{4}\right)^{\frac{1}{2}}$ these four roots p_1, p_2, p_3, p_4 will not be separated as real part and imaginary part explicitly. We only can study the effect of parameter α from the graph. Based on the analysis of the critical values, we get a conclusion that, if $p = p_2$ or $p = p_4$, there will appear three patterns of rogue waves: four-petal state, dark state, bright state. if $p = p_1$ or $p = p_3$, there only exist two patterns: four-petal state and bright state. So the following rogue waves are presented on the choice of $p = p_2$. The approximate classification is:

(a) Four-petal state ($0 \le \alpha < 0.1796$): in this case, (x_2, t_2), (x_3, t_3) are two local maximums, (x_4, t_4), (x_5, t_5) are two local minimums, and (x_1, t_1) is not a local extremum.

(b) Dark state ($0.1796 \le \alpha < 0.6538$): in this case, (x_1, t_1) is the only local minimum and (x_2, t_2), (x_3, t_3) are two local maximums.

(c) Bright state ($\alpha \ge 0.6538$): in this case, (x_1, t_1) is local maximum and (x_4, t_4), (x_5, t_5) are two local minimums (Figs. 1, 2).

Furthermore, the amplitude change at these three critical points is shown in Figs. 3, 4 and 5, respectively, which explain the transformation among these three different states.

In Fig. 3, (a) indicates that these two critical points (x_2, t_2), (x_3, t_3) are maximums, (b) shows that these two critical points (x_4, t_4), (x_5, t_5) are minimums. In addition, the relative amplitude at points (x_2, t_2), (x_3, t_3) is larger than the points (x_4, t_4), (x_5, t_5), which is called the four-petal state.

Then, the generation mechanism of dark rogue wave is depicted in Fig. 4

It is clear that the critical point (x_1, t_1) is minimum, (x_2, t_2), (x_3, t_3) are maximums, and the relative amplitude at (x_1, t_1) is larger than at (x_2, t_2), (x_3, t_3), which generates the dark rogue wave.

The analysis to the bright state is the same as the dark state. Figure 5a only exhibits the first cofactor at (x_1, t_1) due to the order of magnitude to the second cofactor at (x_1, t_1) is too large to exhibit, (a) indicates the critical point (x_1, t_1) is maximum, (x_4, t_4), (x_5, t_5) are minimums, and the relative amplitude at (x_1, t_1) is shorter than at (x_4, t_4), (x_5, t_5), which generates the bright rogue wave.

It is must be emphasized that, when $\alpha < \left(\frac{\left(107+51\sqrt{17}\right)^{\frac{1}{3}}}{12} - \frac{8}{3\left(107+51\sqrt{17}\right)^{\frac{1}{3}}} + \frac{1}{4}\right)^{\frac{1}{2}}$, there exist two patterns, and as the parameter α gets bigger, the rogue wave changes from the four-petal state to dark state. Meanwhile, when $\alpha >$

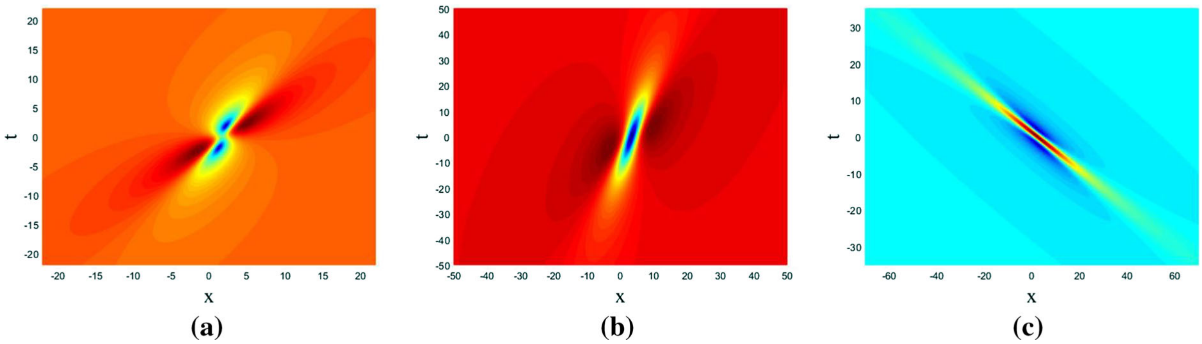

Fig. 2 (Color online) Corresponding density plots of Fig. (1)

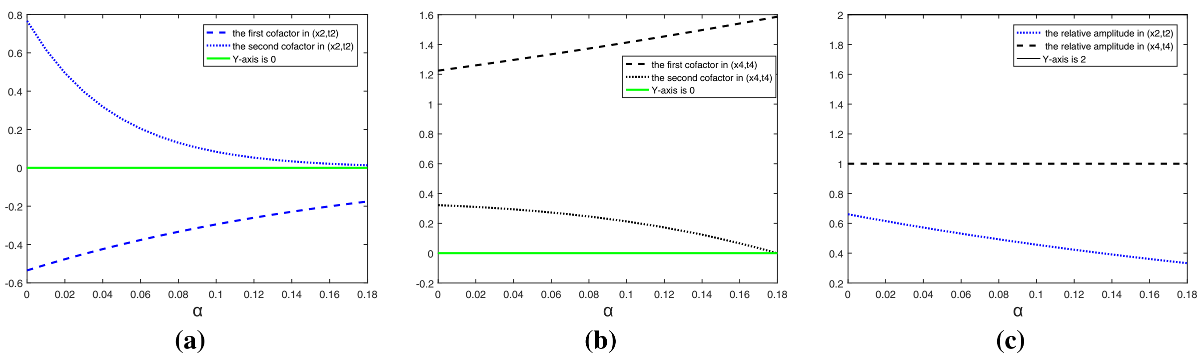

Fig. 3 (Color online) Reason for the generation of four-petal state: **a** the evolution progress of Eqs. 28 and 29 at (x_2, t_2), (x_3, t_3), **b** the evolution progress of Eqs. 28 and 29 at (x_4, t_4), (x_5, t_5), **c** the relative amplitude at these four critical points

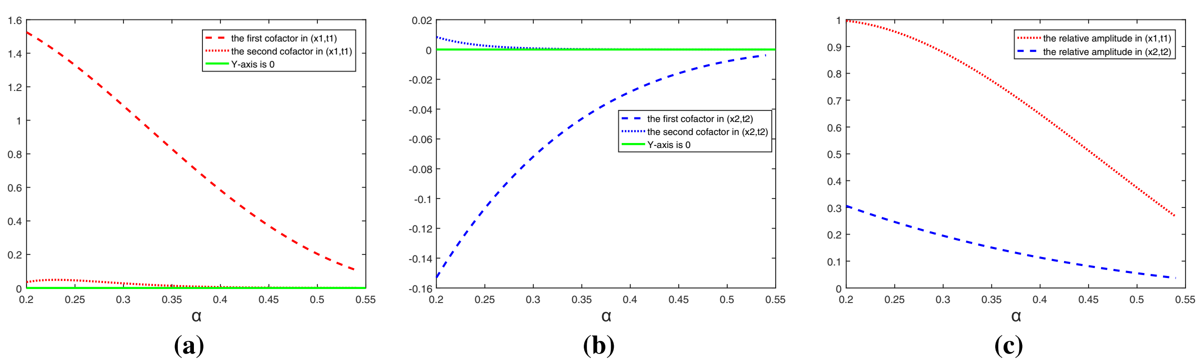

Fig. 4 (Color online) Reason for the generation of dark state: **a** the evolution progress of Eqs. 28 and 29 at (x_1, t_1), **b** the evolution progress of Eqs. 28 and 29 at (x_2, t_2), (x_3, t_3), **c** the relative amplitude at these three critical points

$$\left(\frac{\left(107+51\sqrt{17}\right)^{\frac{1}{3}}}{12}-\frac{8}{3\left(107+51\sqrt{17}\right)^{\frac{1}{3}}}+\frac{1}{4}\right)^{\frac{1}{2}},$$ it only appears the bright rogue wave, but the four-petal state cannot exist. Maybe in this case, if there exists four critical points, it will appear another kind of four-petal rogue wave, evolved from the bright state.

6 High-order rogue waves

The second-order rogue waves can be obtained from Eq. (18) by taking $N = 2$, and the initial values are

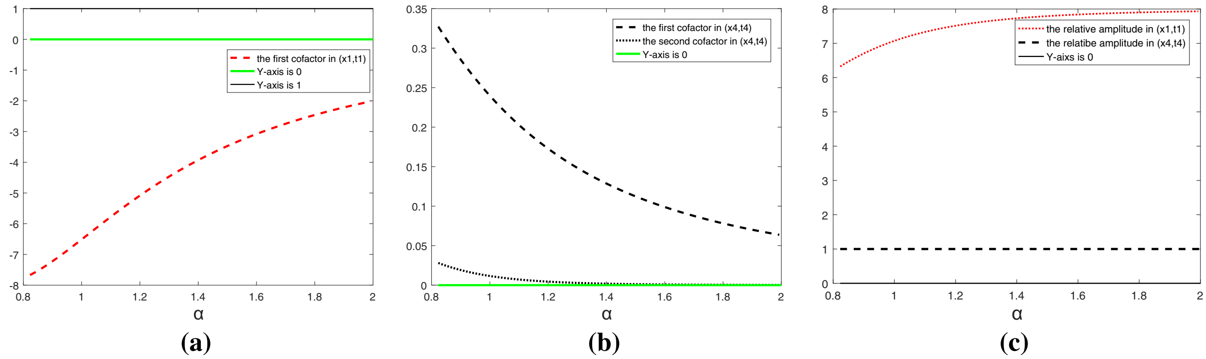

Fig. 5 (Color online) Reason for the generation of bright state: **a** the evolution progress of Eqs. 28 and 29 at (x_1, t_1), **b** the evolution progress of Eqs. 28 and 29 at (x_4, t_4), (x_5, t_5), **c** the relative amplitude at these three critical points

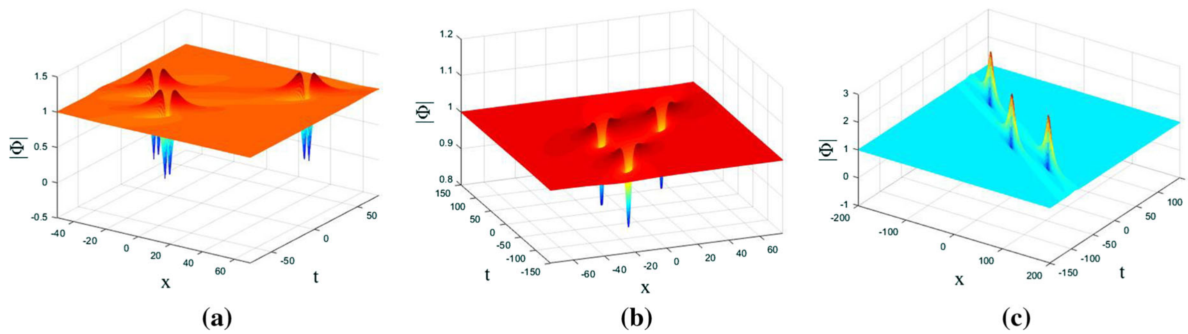

Fig. 6 (Color online) Second-order rogue waves of NLS-Boussinesq equation, **a** the four-petal state for $\alpha = 0, a_3^{(0)} = 500$, **b** dark state for $\alpha = \frac{1}{2}, a_3^{(0)} = 1000$, **c** the bright state for $\alpha = \frac{\sqrt{3}}{2}, a_3^{(0)} = 100 + 10i$

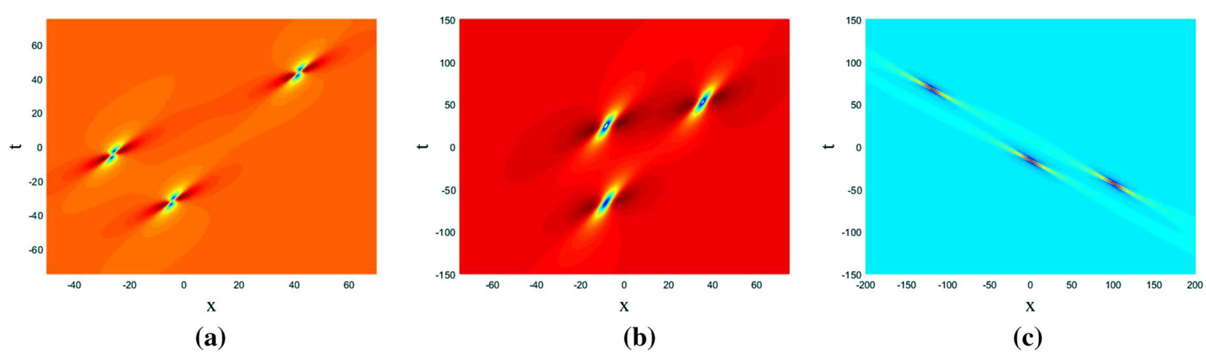

Fig. 7 (Color online) Corresponding density plots of Fig. 6

on the choice of $a_0^{(0)} = 1, a_1^{(0)} = a_2^{(0)} = 0$; then, the functions f, g will be written as

$$f = \begin{vmatrix} m_{11}^{(1,1,0)} & m_{13}^{(1,0,0)} \\ m_{31}^{(0,1,0)} & m_{33}^{(0,0,0)} \end{vmatrix}, \quad g = \begin{vmatrix} m_{11}^{(1,1,1)} & m_{13}^{(1,0,1)} \\ m_{31}^{(0,1,1)} & m_{33}^{(0,0,1)} \end{vmatrix} \tag{30}$$

where

$$\begin{aligned} m_{i,j}^{(\mu,\nu,0)} &= A_i^{(\mu)} B_j^{(\nu)} \frac{1}{p+q} e^{(p+q)x-(p^2-q^2)it}\Big|_{p=\theta,q=\theta^*}, \\ m_{i,j}^{(\mu,\nu,1)} &= -A_i^{(\mu)} B_j^{(\nu)} \frac{1}{p+q} \frac{p-i\alpha}{q+i\alpha} \\ &\quad e^{(p+q)x-(p^2-q^2)it}\Big|_{p=\theta,q=\theta^*}. \end{aligned} \tag{31}$$

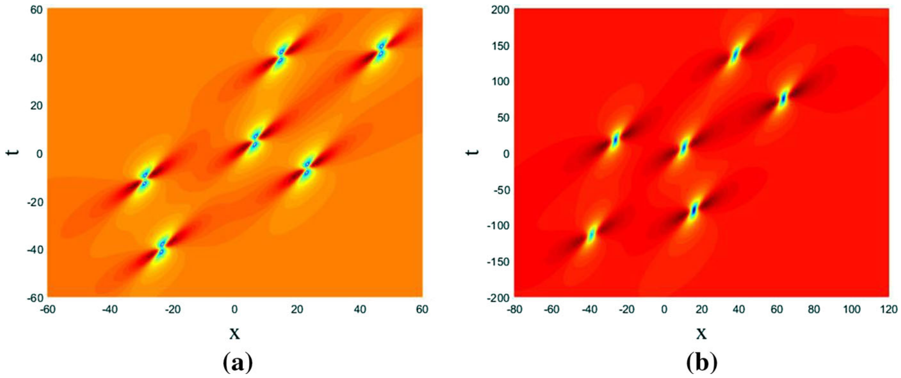

Fig. 8 (Color online) Third-order rogue waves: **a** four-petal state with the choices $\alpha = 0, a_0^{(0)} = 1, a_1^{(0)} = a_2^{(0)} = a_3^{(0)} = a_4^{(0)} = 0, a_5^{(0)} = 1000$, **b** dark state by choosing $\alpha = \frac{1}{2}, a_0^{(0)} = 1, a_1^{(0)} = a_2^{(0)} = a_3^{(0)} = a_4^{(0)} = 0, a_5^{(0)} = 300{,}000$

Similarly, the second-order rogue waves have also three patterns: four-petal state, dark state, bright state, which are depicted in Fig. 6.

Its corresponding density plots are shown in Fig. 7

These three patterns second-order rogue waves (four-petal state, dark state, bright state) all consist of three fundamental first-order rogue waves, and the structures of these three fundamental first-order rogue waves exhibit triangle arrays. In addition, the patterns affected by the parameter α are similar to the fundamental first-order rogue wave, that is, when $0 \leq \alpha < 0.1796$, the second-order rogue wave is four-petal state, when $0.1796 \leq \alpha < 0.6538$, it is the dark rogue wave, when $\alpha > 0.6538$, it is bright rogue wave.

Finally, the four-petal state and dark state of third-order rogue waves are presented in Fig. 8 by choosing some appropriate initial values. But the bright third-order and higher-order rogue waves cannot be exhibited due to the expressions are too complicated to illustrate here.

7 Conclusion

Based on the KP-hierarchy reduction technique, we construct the general high-order rogue waves and analyze the dynamical property of rogue waves, the general formula of N-order rogue waves is given as a determinant form in the theorem and proved by the lemma. The obtained rogue waves exhibit three patterns: four-petal state, dark state and bright state under the extreme value theory, which is governed by a free parameter α. We mainly analyze the Hessian matrix of the function $|\Phi|^2$ with respect to the variables x and t from two cases $k_1 > 0$ and $k_1 < 0$. When $k_1 > 0$, if the function has two maximums and two minimums, it will appear the four-petal state. As the parameter α evolution, the upper relative amplitude is becoming smaller and the lower relative amplitude is bigger, when the critical points number reduces to three, two maximums and one minimum, there appear the dark state. When $k_1 < 0$, the function always has two minimum values and one maximum no matter what the values of parameter α, it appears the bright rogue wave. The theoretical analysis above shows that the different states can be converted by choosing different values of a free parameter α, which provides a favorable theoretical basis to the experiment. In Ref. [21], Zhao et al. studied the transition between the four-petal state and the bright state or the dark state as the change in the relative frequency. But in our paper, the transformation between the bright state and four-petal state is not realized, maybe it is because the upper relative amplitude is smaller than the lower relative amplitude to the four-petal state, which is different from the four-petal state in Ref. [21]. This analysis can be also used to the dynamical behavior of high-order rogue waves for the reason that the high-order rogue waves are the superposition of fundamental rogue waves, such as, the second order is consisted of three fundamental rogue waves and the third order contains six fundamental rogue waves.

As we all know that, by using the Darboux transformation, the interactions between high-order rogue waves and breather or bright–dark soliton are discussed. But as to the Hirota bilinear method and KP-hierarchy reduction technique, there are scarcely any studies about the interaction between the high-order rogue waves and other localized waves. In this paper, we have obtained the high-order rogue waves to the NLS-Boussinesq equation, we should try to focus on the hybrid solutions with the Hirota bilinear method. Furthermore, some nonisospectral equations [50,51] can be discussed by using the similar methods, maybe there will appear some more exciting phenomena. In addition, the rogue wave to discrete integrable system [52,53] is worthy of study.

Acknowledgements We would like to express our sincere thanks to SY Lou, WX Ma, EG Fan, ZY Yan, XY Tang, JC Chen, X Wang and other members of our discussion group for their valuable comments.

Compliance with ethical standards

Conflict of interest The authors declare that there is no conflict of interests regarding the publication of this paper.

Appendix A

In this appendix, we will give the proof to the lemma in Sect. 3 with the KP reduction theory. The detail is as follows:

Proof Based on the solution of the bilinear KP-hierarchy (4), let us bring in the functions with the following form

$$\begin{aligned}\hat{m}^{(n)} &= \frac{1}{p+q}\left(-\frac{p-a}{q+a}\right)^n e^{\gamma+\hat{\gamma}}, \quad \hat{\phi}^{(n)} \\ &= (p-a)^n e^{\gamma}, \quad \hat{\psi}^{(n)} = \left(\frac{-1}{q+a}\right)^n e^{\hat{\gamma}}, \end{aligned} \tag{32}$$

where

$$\begin{aligned}\gamma &= \frac{1}{p-a}x_{-1} + px_1 + p^2x_2 + p^3x_3, \\ \hat{\gamma} &= \frac{1}{q+a} + qx_1 - q^2x_2 + q^3x_3,\end{aligned}$$

in addition, these functions should be satisfied the differential form

$$\begin{aligned}
\partial_{x_1}\hat{m}^{(n)} &= \hat{\phi}^{(n)}\hat{\psi}^{(n)}, \\
\partial_{x_2}\hat{m}^{(n)} &= \left(\partial_{x_1}\hat{\phi}^{(n)}\right)\hat{\psi}^{(n)} - \hat{\phi}^{(n)}\left(\partial_{x_1}\hat{\psi}^{(n)}\right), \\
\partial_{x_3}\hat{m}^{(n)} &= \left(\partial_{x_1}^2\hat{\phi}^{(n)}\right)\hat{\psi}^{(n)} - \left(\partial_{x_1}\hat{\phi}^{(n)}\right)\hat{\psi}^{(n)} \\
&\quad + \hat{\phi}^{(n)}\left(\partial_{x_1}^2\hat{\psi}^{(n)}\right), \\
\partial_{x_{-1}}\hat{m}^{(n)} &= -\hat{\phi}^{(n-1)}\hat{\psi}^{(n+1)}, \\
\hat{m}^{(n+1)} &= \hat{m}^{(n)} + \hat{\phi}^{(n)}\hat{\psi}^{(n+1)}, \\
\partial_{x_2}\hat{\phi}^{(n)} &= \partial_{x_1}^2\hat{\phi}^{(n)}, \\
\partial_{x_3}\hat{\phi}^{(n)} &= \partial_{x_1}^3\hat{\phi}^{(n)}, \\
\hat{\phi}^{(n+1)} &= (\partial_{x_1} - a)\hat{\phi}^{(n)}, \\
\partial_{x_2}\hat{\psi}^{(n)} &= -\partial_{x_1}^2\hat{\psi}^{(n)}, \\
\partial_{x_3}\hat{\psi}^{(n)} &= \partial_{x_1}^3\hat{\psi}^{(n)}, \\
\hat{\psi}^{(n-1)} &= -(\partial_{x_1} + a)\hat{\psi}^{(n)}.
\end{aligned}$$

Then introduce a new entries of the matrix composed by two differential operators:

$$\begin{aligned}\hat{m}_{ij}^{(\mu\nu n)} &= A_i^{(\mu)}B_j^{(\nu)}\hat{m}^{(n)}, \hat{\phi}_i^{(\mu n)} = A_i^{(\mu)}\hat{\phi}^{(n)}, \hat{\psi}_j^{(\nu n)} \\ &= B_j^{(\nu)}\hat{\psi}^{(n)}.\end{aligned}$$

It is clear that the operators A_i^{μ}, B_j^{ν} can commute with the differential operator $\partial_{x_1}, \partial_{x_{-1}}, \partial_{x_2}, \partial_{x_3}$, so these functions are suit for the bilinear KP-hierarchy (3). Furthermore, for an arbitrary $(i_1, i_2, \ldots i_N;\ \mu_1, \mu_2, \ldots, \mu_N, j_1, j_2, \ldots, j_N, \nu_1, \nu_2, \ldots, \nu_N)$, the corresponding determinant

$$\hat{\tau}_n = \det\left(\hat{m}_{i_k, j_l}^{(\mu_k, \nu_l, n)}\right)$$

is satisfied the bilinear KP-hierarchy, especially, when $\hat{\tau}_n = \det_{1\le i,j\le N}\left(\hat{m}_{2i-1,2j-1}^{N-i,N-j,n}\right)$, it is also the solution. Based on the Leibniz rule, one can get

$$\begin{aligned}
&\left[(p-a)\partial_p\right]^m \left(p^3 + \frac{p}{4} - \frac{1}{8(p-a)}\right) \\
&= \sum_{l=0}^{m}\binom{m}{l}\Big[3^l(p-a)^3 + 3a2^l(p-a)^2 \\
&\quad + (3a^2 + \frac{1}{4})(p-a) + (-1)^{l+1}\frac{1}{8(p-a)}\Big] \\
&\quad \left[(p-a)\partial_p\right]^{m-l} + \left(a^3 + \frac{1}{4}a\right)\left[(p-a)\partial_p\right]^m,
\end{aligned} \tag{33}$$

and

$$\begin{aligned}
&\left[(q+a)\partial_q\right]^m \left(q^3 + \frac{q}{4} - \frac{1}{8(q+a)}\right) \\
&= \sum_{l=0}^{m}\binom{m}{l}\Big[3^l(q+a)^3 - 3a2^l(q+a)^2 \\
&\quad + (3a^2 + \frac{1}{4})(q+a) + (-1)^{l+1}\frac{1}{8(q+a)}\Big] \\
&\quad \left[(q+a)\partial_q\right]^{m-l} - \left(a^3 + \frac{1}{4}a\right)\left[(q+a)\partial_q\right]^m.
\end{aligned} \tag{34}$$

Hence, one can obtain the commutator operation

$$
\begin{aligned}
&\left[A_k^{(\mu)}, p^3+\frac{p}{4}-\frac{1}{8(p-a)}\right] \\
&=\sum_{j=0}^{k}\frac{a_j^{(\mu)}}{(k-j)!}\left[\left((p-a)\partial_p\right)^{k-j}, p^3+\frac{p}{4}-\frac{1}{8(p-a)}\right] \\
&=\sum_{j=0}^{k-1}\sum_{l=1}^{k-j}\frac{a_j^{(\mu)}\left[3^l(p-a)^3+3a2^l(p-a)^2+(\frac{12a^2+1}{4})(p-a)+\frac{(-1)^{l+1}}{8(p-a)}\right]\left[(p-a)\partial_p\right]^{k-j-l}}{l!(k-j-l)!}
\end{aligned}
\tag{35}
$$

where [,] devotes the commutator given by $[X, Y]=XY-YX$.

Suppose θ is the solution of the quadratic dispersion equation

$$
3(\theta-a)^3+6a(\theta-a)^2+\left(3a^2+\frac{1}{4}\right)(\theta-a)+\frac{1}{8(\theta-a)}=0, \tag{36}
$$

then the commutator operation equals to zero when $k=0,1$,

$$
\left[A_k^{(\mu)}, p^3+\frac{p}{4}-\frac{1}{8(p-a)}\right]\Bigg|_{p=\theta}=0. \tag{37}
$$

When $k\geq 2$:

Thus, there exists a recurrence relation between the two differential operators

$$
\left[A_k^{(\mu)}, p^3+\frac{p}{4}-\frac{1}{8(p-a)}\right]\Bigg|_{p=\theta}=A_{k-2}^{(\mu+1)}\Big|_{p=\theta},
$$

spontaneously, when $k<0$, this operator $A_k^{(\mu)}=0$.

Similarly, it is obviously that the differential operator $B_l^{(\nu)}$ also satisfies

$$
\left[B_l^{\nu}, q^3+\frac{q}{4}-\frac{1}{8(q+a)}\right]=B_{l-2}^{(\nu+1)}\big|_{q=\theta^*}
$$

when $l>0$, and when $l<0$, we define $B_l^{(\nu)}=0$.

$$
\begin{aligned}
&\left[A_k^{(\mu)}, p^3+\frac{p}{4}-\frac{1}{8(p-a)}\right] \\
&=\sum_{j=0}^{k-2}\sum_{l=2}^{k-j}\frac{a_j^{(\mu)}\left[3^l(p-a)^3+3a2^l(p-a)^2+\left(\frac{12a^2+1}{4}\right)(p-a)+\frac{(-1)^{l+1}}{8(p-a)}\right]\left[(p-a)\partial_p\right]^{k-j-l}}{l!(k-j-l)!}\Bigg|_{p=\theta} \\
&=\sum_{j=0}^{k-2}\sum_{\tilde{l}=0}^{k-j-2}\frac{a_j^{\mu}\left[3^{\tilde{l}+2}(p-a)^3+3a2^{\tilde{l}+2}(p-a)^2+\left(\frac{12a^2+1}{4}\right)(p-a)+\frac{(-1)^{\tilde{l}+1}}{8(p-a)}\right]\left[(p-a)\partial_p\right]^{k-j-\tilde{l}-2}}{(\tilde{l}+2)!(k-j-\tilde{l}-2)!}\Bigg|_{p=\theta} \\
&=\sum_{\hat{j}=0}^{k-2}\left(\sum_{\hat{l}=0}^{\hat{j}}\frac{3^{\hat{l}+2}(p-a)^3+3a2^{\hat{l}+2}(p-a)^2+\left(\frac{12a^2+1}{4}\right)(p-a)+\frac{(-1)^{\hat{l}+1}}{8(p-a)}}{(\hat{l}+2)!}a_{\hat{j}-\hat{l}}^{(\mu)}\right)\frac{\left((p-a)\partial_p\right)^{k-2-\hat{j}}}{(k-2-\hat{j})!}\Bigg|_{p=\theta} \\
&=\sum_{\hat{j}=0}^{k-2}a_{\hat{j}}^{(\mu+1)}\frac{\left((p-a)\partial_p\right)^{k-2-\hat{j}}}{(k-2-\hat{j})!}\Bigg|_{p=\theta}=A_{k-2}^{(\mu+1)}\big|_{p=\theta}.
\end{aligned}
\tag{38}
$$

Under the above two recurrence equation, the following derivative relation can be derived as:

$$\begin{aligned}
&\left(\partial_{x_3}+\frac{1}{4}\partial_{x_1}-\frac{1}{8}\partial_{x_{-1}}\right)\hat{m}_{kl}^{(\mu\nu n)}\Big|_{p=\theta,q=\theta^*}\\
&=\Bigg(A_k^{(\mu)}B_l^{(\nu)}\bigg(p^3+q^3+\frac{1}{4}(p+q)\\
&\quad-\frac{1}{8}\left(\frac{1}{p-a}+\frac{1}{q+a}\right)\bigg)\hat{m}^{(n)}\Bigg)\Big|_{p=\theta,q=\theta^*}\\
&=\left(A_k^{(\mu)}\left(p^3+\frac{p}{4}-\frac{1}{8(p-a)}\right)\right.\\
&\quad\left.B_l^{(\nu)}\hat{m}^{(n)}\right)\Big|_{p=\theta,q=\theta^*}\\
&\quad+\left(A_k^{(\mu)}B_l^{(\nu)}\left(q^3+\frac{q}{4}-\frac{1}{8(q+a)}\right)\right.\\
&\quad\left.\hat{m}^{(n)}\right)\Big|_{p=\theta,q=\theta^*}\\
&=\Bigg(\Bigg(\left(\left((p^3+\frac{p}{4}-\frac{1}{8(p-a)})A_k^{(\mu)}\right)\right.\\
&\quad\left.+A_{k-2}^{(\mu+1)}\right)B_l^{(\nu)}\hat{m}^{(n)}\Bigg)\Big|_{p=\theta,q=\theta^*}\\
&\quad+\left(A_k^{(\mu)}\left(\left(\left(\left(q^3+\frac{q}{4}-\frac{1}{8(q+a)}\right)B_l^{(\nu)}\right)\hat{m}^{(n)}\right)\right.\right.\\
&\quad\left.\left.+B_{l-2}^{\nu+1}\right)\right)\Big|_{p=\theta,q=\theta^*}\\
&=\left(p^3+\frac{p}{4}-\frac{1}{8(p-a)}\right)\hat{m}_{kl}^{(\mu\nu n)}\Big|_{p=\theta,q=\theta^*}\\
&\quad+\hat{m}_{k-2,l}^{(\mu+1,\nu,n)}\Big|_{p=\theta,q=\theta^*}\\
&\quad+\left(q^3+\frac{q}{4}-\frac{1}{8(q+a)}\right)\hat{m}_{kl}^{(\mu\nu n)}\Big|_{p=\theta,q=\theta^*}\\
&\quad+\hat{m}_{k,l-2}^{(\mu,\nu+1,n)}\Big|_{p=\theta,q=\theta^*}.
\end{aligned}\tag{39}$$

Once more, based on the above relation, the differential form of a special determinant rewritten as

$$\hat{\hat{\tau}}_n=\det_{1\le i,j\le N}\left(\hat{m}_{2i-1,2j-1}^{N-i,N-j,n}\big|_{p=\theta,q=\theta^*}\right)\tag{40}$$

can be worked out as

$$\begin{aligned}
&\left(\partial_{x_3}+\frac{1}{4}\partial_{x_1}-\frac{1}{8}\partial_{x_{-1}}\right)\hat{\hat{\tau}}_n\\
&=\sum_{i=1}^{N}\sum_{j=1}^{N}\triangle_{ij}\left(\partial_{x_3}+\frac{1}{4}\partial_{x_1}-\frac{1}{8}\partial_{x_{-1}}\right)\\
&\quad\left(\hat{m}_{2i-1,2j-1}^{N-1,N-j,n}\Big|_{p=\theta,q=\theta^*}\right)\\
&=\sum_{i=1}^{N}\sum_{j=1}^{N}\triangle_{ij}\Bigg[\left(p^3+\frac{p}{4}-\frac{1}{8(p-a)}\right)\\
&\quad\hat{m}_{2i-1,2j-1}^{(N-i,N-jn)}\Big|_{p=\theta,q=\theta^*}\\
&\quad+\hat{m}_{2i-3,2j-1}^{(N-i+1,N-j,n)}\Big|_{p=\theta,q=\theta^*}\\
&\quad+\left(q^3+\frac{q}{4}-\frac{1}{8(q+a)}\right)\hat{m}_{2i-1,2j-1}^{(N-i,N-jn)}\Big|_{p=\theta,q=\theta^*}\\
&\quad+\hat{m}_{2i-1,2j-3}^{(N-i,N-j+1,n)}\Big|_{p=\theta,q=\theta^*}\Bigg]\\
&=\left(p^3+\frac{p}{4}-\frac{1}{8(p-a)}\right)N\hat{\hat{\tau}}_n\Big|_{p=\theta,q=\theta^*}\\
&\quad+\sum_{i=1}^{N}\sum_{j=1}^{N}\triangle_{ij}\hat{m}_{2i-3,2j-1}^{(N-i+1,N-j,n)}\Big|_{p=\theta,q=\theta^*}\\
&\quad+\left(q^3+\frac{q}{4}-\frac{1}{8(q+a)}\right)N\hat{\hat{\tau}}_n\Big|_{p=\theta,q=\theta^*}\\
&\quad+\sum_{i=1}^{N}\sum_{j=1}^{N}\triangle_{ij}\hat{m}_{2i-1,2j-3}^{(N-i,N-j+1,n)}\Big|_{p=\theta,q=\theta^*},
\end{aligned}\tag{41}$$

where $\triangle_{ij}$ is the (i,j)-cofactor of the matrix $\left(\hat{m}_{2i-1,2j-1}^{N-i,N-j,n}\right)$. It is obvious that $\sum_{i=1}^{N}\sum_{j=1}^{N}\triangle_{ij}$ $\hat{m}_{2i-3,2j-1}^{(N-i+1,N-j,n)}\big|_{p=\theta,q=\theta^*}=0$ for $\triangle_{ij}$ is the (i,j)-cofactor of the matrix $\left(\hat{m}_{2i-1,2j-1}^{N-i,N-j,n}\right)$ but not the $\left(\hat{m}_{2i-3,2j-1}^{N-i+1,N-j,n}\right)$. Similarly, $\sum_{i=1}^{N}\sum_{j=1}^{N}\triangle_{ij}$ $\hat{m}_{2i-1,2j-3}^{(N-i,N-j+1,n)}\big|_{p=\theta,q=\theta^*}=0$. Therefore, Eq. (41) will be changed into

$$\left(\partial_{x_3}+\frac{1}{4}\partial_{x_1}-\frac{1}{8}\partial_{x_{-1}}\right)\hat{\hat{\tau}}_n = \left(p^3+\frac{p}{4}-\frac{1}{8(p-a)}+q^3+\frac{q}{4}-\frac{1}{8(q+a)}\right)N\hat{\hat{\tau}}_n. \tag{42}$$

Due to $\hat{\hat{\tau}}_n$ is a special case of $\hat{\tau}_n$, so $\hat{\hat{\tau}}_n$ is the solution to the $(1+1)$-dimensional bilinear equation:

$$\begin{aligned}&\left(D_{x_1}^2+2aD_{x_1}-D_{x_2}\right)\hat{\hat{\tau}}_{n+1}\cdot\hat{\hat{\tau}}_n=0,\\&\left(D_{x_1}^2+D_{x_1}^4+3D_{x_2}^2-1\right)\hat{\hat{\tau}}_n\cdot\hat{\hat{\tau}}_n+\hat{\hat{\tau}}_{n+1}\cdot\hat{\hat{\tau}}_{n-1}=0.\end{aligned} \tag{43}$$

Under reduction Eq. (42), these variables x_{-1}, x_3 in $\hat{\hat{\tau}}_n$ will become dummy. Thus, the matrix entries $\hat{m}_{2N-i,2N-j}^{(N-i,N-j,n)}$ reduce to $m_{2N-i,2N-j}^{(N-i,N-j,n)}$, τ_n in Eq. (11) satisfy Eq. (6), and the proof is completed. □

References

1. Onorato, M., Osborne, A.R., Srio, M.: Modulational instability in crossing sea states: a possible mechanism for the formation of freak waves. Phys. Rev. Lett. **96**, 014503 (2006)
2. Baronio, F., Conforti, M., Degasperis, A., Lombardo, S., Onorato, M., Wabnitz, S.: Vector rogue waves and baseband modulation instability in the defocusing regime. Phys. Rev. Lett. **113**, 034101 (2014)
3. Peterson, P., Soomere, T., Engelbrecht, J., Groesen, E.V.: Soliton interaction as a possible model for extreme waves in shallow water. Nonlinear Process. Geophys. **10**, 503–510 (2003)
4. Pelinovsky, E., Kharif, C., Talipova, T.: Large-amplitude long wave interaction with a vertical wall. Eur. J. Mech. B Fluid **27**, 409–418 (2008)
5. Solli, D.R., Ropers, C., Koonath, P., Jalali, B.: Optical rogue waves. Nature **450**, 1054–1058 (2007)
6. Pierangeli, D., Mei, F.D., Conti, C., Agranat, A.J., DelRe, E.: Spatial rogue waves in photorefractive ferroelectrics. Phys. Rev. Lett. **115**, 093901 (2015)
7. Akhmediev, N., Dudley, J.M., Solli, D.R., Turitsyn, S.K.: Recent progress in investigating optical rogue waves. J. Opt. **15**, 060201 (2013)
8. Bludov, Y.V., Konotop, V.V., Akhmediev, N.: Matter rogue waves. Phys. Rev. A **80**, 033610 (2009)
9. Moslem, W.M.: Langmuir rogue wave in electron–positron plasmas. Phys. Plasmas **18**, 032301 (2011)
10. Yan, Z.Y.: Vector financial rogue waves. Phys. Lett. A **375**, 4274–4279 (2011)
11. Ohta, Y., Yang, J.K.: Genera high-order rogue wvae and their dynamics in the nonlinear Schrödinger equation. Proc. R. Soc. Lond. Sect. A **468**, 1716–1740 (2012)
12. Akhmediev, N., Ankiewicz, A., Soto-Crespo, J.M.: Rogue waves and rational solutions of the nonlinear Schrödinger equation. Phys. Rev. E **80**, 026601 (2009)
13. Guo, B.L., Ling, L.M., Liu, Q.P.: High-order solution and generalized Darboux transformation of derivative nonlinear Schrödinger equation. Stud. Appl. Math. **130**, 317–344 (2012)
14. Ling, L.M., Guo, B.L., Zhao, L.C.: High-order rogue waves in vector nonlinear Schrödinger equation. Phys. Rev. E **89**, 041201 (2014)
15. Xu, S.W., He, J.S., Wang, L.H.: The Darboux transformation of the derivative nonlinear Schrödinger equation. J. Phys. A Math. Theor. **44**, 305203 (2011)
16. Wang, Y.Y., Liang, C., Dai, C.Q., Zheng, J., Fan, Y.: Exact vector multipole and vortex solitons in the media with spatially modulated cubic–quintic nonlinearity. Nonlinear Dyn. **90**, 1269–1275 (2017)
17. Dai, C.Q., Zhou, G.Q., Chen, R.P., Lai, X.J., Zheng, J.: Vector multipole and vortex solitons in two-dimensional Kerr media. Nonlinear Dyn. **88**, 2629–2635 (2017)
18. Dai, C.Q., Wang, Y.Y., Fan, Y., Yu, D.G.: Reconstruction of stability for Gaussian spatial solitons in quintic–septimal nonlinear materials under PT-symmetric potentials. Nonlinear Dyn. **92**, 1351–1358 (2018)
19. Peregrine, D.H.: Water waves, nonlinear Schrödinger equations and their solutions. J. Aust. Math. Soc. B **25**, 16–43 (1983)
20. Kibler, B., Fatome, J., Finot, C., Millot, G., Dias, F., Genty, G., Akhmediev, N., Dudley, J.M.: The peregrine soliton in nonlinear fibre optics. Nat. Phys. **6**, 790–795 (2010)
21. Zhao, L.C., Xin, G.G., Yang, Z.Y.: Rogue-wave pattern transition induced by relative frequency. Phys. Rev. E **90**, 022918 (2014)
22. Chabchoub, A., Hoffmann, N., Onorato, M., Slunyaev, A., Sergeeva, A., Pelinovsky, E., Akhmediev, N.: Observation of hierarchy of up to fifth-order rogue waves in a water tank. Phys. Rev. E **86**, 056601 (2012)
23. Guo, B.L., Ling, L.M.: Rogue wave, breathers and bright–dark-rogue solutions for the coupled Schrödinger equations. Chin. Phys. Lett. **28**, 110202 (2011)
24. Zhang, G.Q., Yan, Z.Y., Wen, X.Y., Chen, Y.: Interactions of localized wave structures and dynamics in the defocusing coupled nonlinear Schrödinger equations. Phys. Rev. E **95**, 042201 (2017)
25. Xu, T., Chen, Y., Lin, J.: Localized waves of the coupled cubic-quintic nonlinear Schrödinger equations in nonlinear optics. Chin. Phys. B **26**, 120200 (2017)
26. Wei, J., Wang, X., Geng, X.G.: Periodic and rational solutions of the reduced Maxwell–Bloch equations. Commun. Nonlinear Sci. Numer. Simul. **59**, 1–14 (2017)
27. Liu, Y.K., Li, B., An, H.L.: General high-order breathers, lumps in the (2 + 1)-dimensional Boussinesq equation. Nonlinear Dyn. (2018). https://doi.org/10.1007/s11071-018-4181-6
28. Zhang, X.E., Chen, Y., Tang, X.Y.: Rogue wave and a pair of resonance stripe solitons to a reduced generalized (3 + 1)-dimensional KP equation. arXiv:1610.09507
29. Zhang, X.E., Chen, Y.: Rogue wave and a pair of resonance stripe solitons to a reduced (3 + 1)-dimensional Jimbo–Miwa equation. Commun. Nonlinear Sci. Numer. Simul. **52**, 24–31 (2017)

30. Zhang, X.E., Chen, Y.: Deformation rogue wave to the (2 + 1)-dimensional KdV equation. Nonlinear Dyn. **90**, 755–763 (2017)
31. Jimbo, M., Miwa, T.: Solitons and infinite dimensional Lie algebras. Publ. RIMS Kyoto Univ. **19**, 943–1001 (1983)
32. Ohta, Y.: Wronskian solutions of soliton equations. RIMS kôkyûroku **684**, 1–17 (1989)
33. Ohta, Y., Wang, D.S., Yang, J.K.: General N-dark–dark solitons in the coupled nonlinear Schrödinger equations. Stud. Appl. Math. **127**, 345–371 (2011)
34. Feng, B.F.: General N-soliton solution to a vector nonlinear Schrödinger equation. J. Phys. A Math. Theor. **47**, 355203 (2014)
35. Ling, L.M., Zhao, L.C., Guo, B.L.: Darboux transformation and multi-dark soliton for N-component nonlinear Schrödinger equations. Nonlinearity **28**, 3243–3261 (2015)
36. Chen, J.C., Chen, Y., Feng, B.F., Maruno, K.I., Ohta, Y.: An integrable semi-discretization of the coupled Yajima–Oikawa system. J. Phys. A Math. Theor. **49**, 165201 (2016)
37. Chen, J.C., Chen, Y., Feng, B.F., Maruno, K.I., Ohta, Y.: General high-order rogue waves of the (1 + 1)-dimensional Yajima–Oikawa system. arXiv:1709.03781
38. Chen, J.C., Chen, Y., Feng, B.F., Maruno, K.I.: Rational solutions to two-and one-dimensional multicomponent Yajima–Oikawa systems. Phys. Lett. A **379**, 1510–1519 (2015)
39. Chen, J.C., Feng, B.F., Chen, Y., Ma, Z.Y.: General bright–dark soliton solutions to (2 + 1)-dimensional multi-component long-wave–short-wave resonance interaction system. Nonlinear Dyn. **88**, 1–16 (2017)
40. Han, Z., Chen, Y., Chen, J.C.: General N-dark soliton solutions of the multi-component Mel'nikov system. J. Phys. Soc. Jpn. **86**, 074005 (2017)
41. Han, Z., Chen, Y., Chen, J.C.: Bright-dark mixed N-soliton solutions of the multi-component mel'nikov system. J. Phys. Soc. Jpn. **86**, 104008 (2017)
42. Sun, B.N., Wazwaz, A.M.: Interaction of lumps and dark solitons in the Mel'nikov equation. Nonlinear Dyn. (2018). https://doi.org/10.1007/s11071-018-4180-7
43. Wazwaz, A.M.: Multiple soliton solutions and multiple complex soliton solutions for two distinct Boussinesq equations. Nonlinear Dyn. **85**, 731–737 (2016)
44. Wazwaz, A.M., El-Tantawy, S.A.: Solving the (3 + 1)-dimensional KP-Boussinesq and BKP-Boussinesq equations by the simplified Hirota's method. Nonlinear Dyn. **88**, 3017–3021 (2017)
45. Rao, N.N.: Exact solutions of coupled scalar field equations. J. Phys. A Math. Gen. **22**, 4813–4825 (1989)
46. Singh, S.V., Rao, N.N., Shukla, P.K.: Nonlinearly coupled Langmuir and dust-acoustic waves in a dusty plasma. J. Plasma Phys. **3**, 551–567 (1998)
47. Hase, Y., Satsuma, J.: An N-soliton solutions for the nonlinear Schrödinger equation coupled to the Boussinesq equation. J. Phys. Soc. Jpn. **57**, 679–682 (1988)
48. Mu, G., Qin, Z.Y.: Rogue waves for the coupled Schrödinger–Boussinesq equation and the coupled higgs equation. J. Phys. Soc. Jpn. **81**, 084001 (2012)
49. Lu, C.N., Fu, C., Yang, H.W.: Time-fractional generalized Boussinesq equation for Rossby solitary waves with dissipation effect in stratified fluid and conservation laws as well as exact solutions. Appl. Math. Comput. **327**, 104–116 (2018)
50. Xu, X.X.: An integrable coupling hierarchy of the Mkdv-integrable systems, its hamiltonian structure and corresponding nonisospectral integrable hierarchy. Appl. Math. Comput. **216**, 344–353 (2010)
51. Xu, T., Chen, Y.: Darboux transformation of the coupled nonisospectral Gross–Pitaevskii system and its multi-component generalization. Commun. Nonlinear Sci. Numer. Simul. **57**, 276–289 (2018)
52. Tang, L.Y., Fan, J.C.: A family of liouville integrable lattice equations and its conservation laws. Appl. Math. Comput. **217**, 1907–1912 (2010)
53. Li, X.Y., Li, Y.X., Yang, H.X.: Two families of liouville integrable lattice equations. Appl. Math. Comput. **217**, 8671–8682 (2011)